

# Diffusion process in enzyme–metal hybrid catalysts

Shitong Cui<sup>1</sup>, Jun Ge (✉)<sup>1,2</sup>

<sup>1</sup> Key Lab for Industrial Biocatalysis, Ministry of Education, Department of Chemical Engineering, Tsinghua University, Beijing 100084, China

<sup>2</sup> Institute of Biopharmaceutical and Health Engineering, Tsinghua Shenzhen International Graduate School, Shenzhen 518055, China

© Higher Education Press 2022

**Abstract** Enzyme–metal hybrid catalysts bridge the gap between enzymatic and heterogeneous catalysis, which is significant for expanding biocatalysis to a broader scope. Previous studies have demonstrated that the enzyme–metal hybrid catalysts exhibited considerably higher catalytic efficiency in cascade reactions, compared with that of the combination of separated enzyme and metal catalysts. However, the precise mechanism of this phenomenon remains unclear. Here, we investigated the diffusion process in enzyme–metal hybrid catalysts using Pd/lipase-Pluronic conjugates and the combination of immobilized lipase (Novozyme 435) and Pd/C as models. With reference to experimental data in previous studies, the Weisz–Prater parameter and efficiency factor of internal diffusion were calculated to evaluate the internal diffusion limitations in these catalysts. Thereafter, a kinetic model was developed and fitted to describe the proximity effect in hybrid catalysts. Results indicated that the enhanced catalytic efficiency of hybrid catalysts may arise from the decreased internal diffusion limitation, size effect of Pd clusters and proximity of the enzyme and metal active sites, which provides a theoretical foundation for the rational design of enzyme–metal hybrid catalysts.

**Keywords** enzyme–metal hybrid catalyst, internal diffusion, proximity effect, kinetic model

## 1 Introduction

Enzymes have been widely used as catalysts in the synthesis of organic compounds, particularly in asymmetric catalysis to form chiral structures, which has provided appealing advantages such as high selectivity, mild condition, and green process [1–3]. Chemical catalysis, such as metal catalysis, is extensively applied in industry

because metal catalysts are more adaptive to harsh conditions such as high temperature, high pressure, extreme pH, organic solvents, and exhibit high catalytic efficiency under these conditions [4,5]. Enzyme–metal hybrid catalysts (EMHCs) which integrate biocatalysis and chemical catalysis have become an emerging topic in catalytic research for the past few years [6,7] because this integration can combine the specific selectivity of biocatalysts and the excellent reactivity of chemical catalysts in one pot, rather than the sequential arrangement of individual catalysts, thus reducing the cost for the separation of intermediates and improving the overall efficiency. However, a major challenge in this one-pot catalytic process is the incompatibility between enzymes and metal catalysts because the optimal conditions for these two types of catalysts are quite different as mentioned above [8]. Recently, with the rapid development in material science, a possible strategy to overcome this issue may be the rational design of enzyme–metal interfaces to control their structures and adjust their properties so as to better match the catalysts [9]. Therefore, various types of EMHCs have been constructed and applied in different fields [10–12].

A typical reaction catalyzed by EMHCs is the dynamic kinetic resolution (DKR) of enantiomers which is a powerful tool for the synthesis of enantiomerically pure alcohols or amines. In this reaction, the kinetic resolution of racemic mixtures is catalyzed by enzymes and the racemization of the unconsumed enantiomer is catalyzed by metal nanoparticles (NPs) [13–17]. Therefore, combined with the *in situ* racemization, the resolution process has a theoretical yield of 100% [18]. For example, our lab has developed an approach to construct EMHCs, using the *Candida antarctica* lipase B (CALB)-polymer conjugates as the confined nanoreactor for the *in situ* generation of Pd NPs [19]. The as-synthesized Pd/CALB-Pluronic (Pd/CALB-P) exhibited an excellent catalytic performance during the DKR of (±)-1-phenylethylamine ((±)-1-PEA), demonstrating a 7.6-time efficiency, compared with the combination of commercial immobilized lipase Novozyme 435 and Pd/C. This phenomenon is similar to that in a study conducted by Bäckvall group

Received July 28, 2021; accepted November 15, 2021

E-mail: junge@mail.tsinghua.edu.cn

[20], in which lipase and Pd NPs were coimmobilized in the cavities of siliceous mesocellular foam (MCF) (denoted as Pd/CALB-AmP-MCF). The Pd/CALB-AmP-MCF catalyst achieved a conversion rate of 95% at 70 °C after 16 h in the DKR of ( $\pm$ )-1-PEA, while 24 h was nearly required to realize a similar conversion when the combination of Pd-AmP-MCF and Novozyme 435 was used [21]. Moreover, Zhang et al. [22] reported a method to develop EMHCs based on a core-shell design in which Pd NPs were loaded onto the aminopropyl group modified mesoporous silica nanosphere (Pd/NH<sub>2</sub>-MSN) as the inner core and the enzyme was adsorbed on the porous outer shell. The as-synthesized Pd/NH<sub>2</sub>-MSN@BTME@CALB/L-mesosilica hybrid catalyst demonstrated a higher efficiency in the DKR of chiral amines than that of the separated counterparts. Hence, despite the various strategies to develop EMHCs, it seems to appear a general phenomenon that the efficiency of EMHCs to catalyze DKR reactions in one pot tends to be higher than that of the separated counterparts. In addition, this phenomenon was also observed in other hybrid catalysts and cascade reactions such as the multi-enzyme system [23–25]. Several attempts have been made from various perspectives to elucidate the enhanced activity of EMHCs, including the size effect of Pd NPs [19], proximity of enzyme and metal active sites [26], and the microenvironment of catalysts [27].

However, to the best of our knowledge, it is still challenging to understand the catalytic performance of EMHCs from the viewpoint of heterogeneous catalysis, which is an important aspect in chemical reaction engineering. Here, based on available data in previous studies and basic theories of reaction engineering, a calculative analysis was conducted to investigate the diffusion

process in EMHCs, using the Pd/CALB-P developed by our group [19] as the model and the combination of Pd/C and Novozyme 435 for comparison. A mechanism of internal diffusion in heterogeneous catalysis was proposed to describe the diffusion process of reactants from the bulk solution to the active sites. Thereafter, kinetic analysis was used to describe the diffusion of intermediates between the active sites of the metal and enzyme. We expect that the analysis from the perspective of reaction engineering would be helpful for a deeper understanding and precise design of EMHCs.

## 2 Model development

Schematics in Fig. 1 demonstrate the process focused on in this study. The cascade reaction (such as the DKR process) catalyzed by Pd/CALB-P or the combination of Pd/C and Novozyme 435 is heterogeneous or pseudo-homogeneous catalysis. Figure 1(a) illustrates a typical heterogeneous catalysis comprising seven steps including the 1) diffusion of reactants from the bulk solution to the external surface of catalysts, 2) diffusion of reactants from the external surface to the active sites, 3) adsorption of reactants on the active sites, 4) catalytic reaction, 5) desorption of products from the active sites, 6) diffusion of products from the active sites to the external surface of catalysts and 7) diffusion of products from the external surface to the bulk solution. Among them, steps 1), 2), 6) and 7) can be classified into external diffusion (steps 1) and 7)) and internal diffusion (steps 2) and 6)), while steps 3), 4), and 5) belong to the reaction process. In

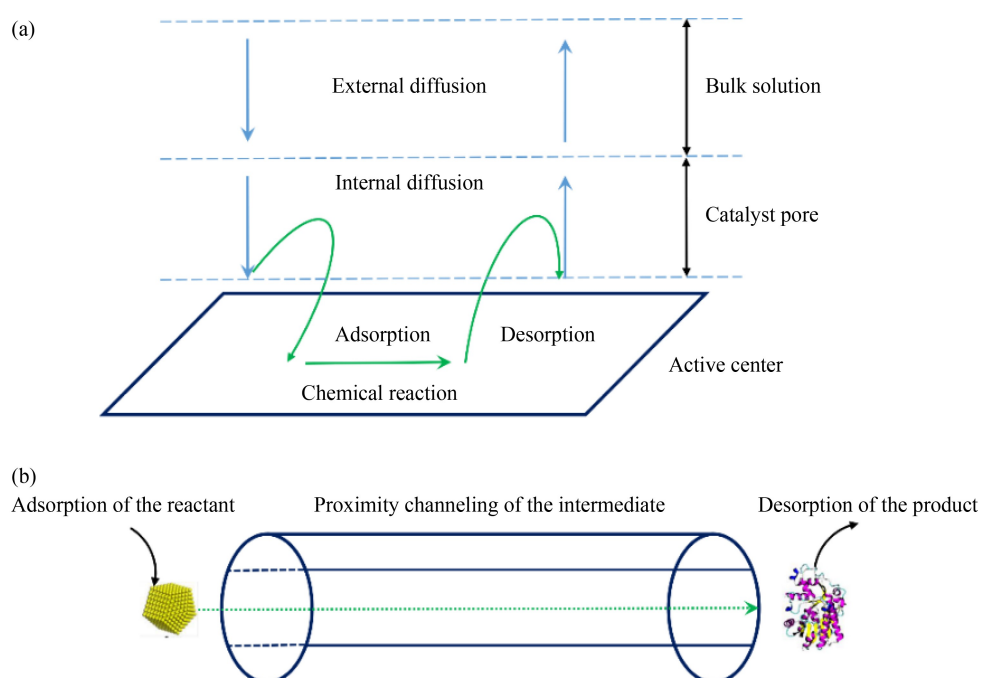


**Fig. 1** Schematics showing the process of (a) the heterogeneous catalysis and (b) the proximity channeling effect.

certain cases, when the rate of diffusion is lower than the rate of reaction, the whole process tends to be diffusion-limited. Thus, the evaluation of the diffusion effect during the catalytic process is an essential consideration in heterogeneous catalysis. Besides, for cascade reactions, the transport of intermediates between active sites (Fig. 1(b)) is considered to be a key factor affecting the throughput of cascade reactions. The confined environment in EMHCs might partly prevent intermediates from diffusing to the bulk solution, thus increasing the throughput, known as the “proximity channeling” effect [26]. Therefore, two issues will be investigated in this study: 1) the internal diffusion effect and 2) the proximity channeling effect, during the DKR process catalyzed by Pd/CALB-P and the combination of Novozyme 435 and Pd/C.

## 2.1 Global assumptions

Several assumptions are proposed as follows: 1) Catalysts analyzed in this study are all treated as spherical particles. 2) The effect of external diffusion can be disregarded when the reaction system is intensively stirred. 3) There is no accumulation of intermediates in the system (i.e., the generating rate is equal to the consumption rate). 4) Reactions catalyzed by Pd NPs are first-order to substrates [28]. 5) Reactions catalyzed by CALB are second-order to substrates (discussed below).

## 2.2 Evaluation of the internal diffusion limitations

In most cases, the stirring rate in the DKR process will be sufficiently fast to disregard the effect of external diffusion [19]. Therefore, according to the second assumption in section 2.1, the internal diffusion will be dominant when reactants are diffusing from the bulk solution to the active sites.

Generally, for spherical particles, the effect of internal diffusion can be evaluated using the Weisz–Prater criterion [29]:

$$C_{WP} = \frac{-r'(\text{obs})\rho_c R^2}{D_e C_s}, \quad (1)$$

where  $C_{WP}$  indicates the ratio of the reaction rate to the diffusion rate, where the internal diffusion effect can be disregarded with  $C_{WP} \ll 1$  and the internal diffusion will be dominant when  $C_{WP} > 1$ . In addition, the internal diffusion limitations in catalysts can also be compared by the efficiency factor of internal diffusion  $\eta$ :

$$\eta = \frac{3}{\varphi^2} (\varphi \coth \varphi - 1), \quad (2)$$

where  $\varphi$  is the Thiele modulus of catalysts. The efficiency factor of internal diffusion  $\eta$  refers to the ratio of the observed activity to the intrinsic activity. Therefore, a high  $\eta$  indicates a weak effect of internal diffusion. Moreover,  $C_{WP}$ ,  $\eta$  and  $\varphi$  can be correlated as follows:

$$C_{WP} = \varphi^2 \eta. \quad (3)$$

Equation (3) indicates that  $\eta$  can be calculated by trial and error when the value of  $C_{WP}$  is known.

The effective diffusion coefficient  $D_e$  of reactants can be obtained by [30]:

$$\frac{1}{D_e} = \frac{1}{D_{12,\text{eff}}} + \frac{1}{D_{K,\text{eff}}}, \quad (4)$$

where  $D_{12,\text{eff}}$  is the effective coefficient of molecular diffusion, defined as follows:

$$D_{12,\text{eff}} = \frac{D_{12}\theta}{\tau}, \quad (5)$$

where the molecular diffusion coefficient  $D_{12}$  of the reactants in a dilute solution can be estimated using the Wikle–Chang empirical equation:

$$D_{12} = 7.4 \times 10^{-10} \frac{T(XM)^{1/2}}{\mu V_b^{0.6}}. \quad (6)$$

$D_{K,\text{eff}}$  is the effective coefficient of the Knudsen diffusion which is used to describe the diffusion in porous materials with small pore sizes:

$$D_{K,\text{eff}} = \frac{9700 r_e}{\tau} \sqrt{\frac{T}{M}}. \quad (7)$$

All the parameters used in this model are listed in Table 1.

**Table 1** Parameters used in the model

Symbol	Description	Unit
$C_{WP}$	Weisz–Prater parameter	1
$\eta$	Efficiency factor of internal diffusion	1
$\varphi$	Thiele modulus	1
$D_e$	Effective diffusion coefficient	$\text{cm}^2 \cdot \text{s}^{-1}$
$D_{12}$	Molecular diffusion coefficient	$\text{cm}^2 \cdot \text{s}^{-1}$
$D_K$	Knudsen diffusion coefficient	$\text{cm}^2 \cdot \text{s}^{-1}$
$\rho_c$	Particle density	$\text{g} \cdot \text{cm}^{-3}$
$R$	Particle size	cm
$\theta$	Porosity of the catalysts	1
$\tau$	Tortuosity of the catalysts	1
$r_e$	Average pore size	cm
$r'(\text{obs})$	Observed reaction rate	$\text{mol} \cdot \text{g}^{-1} \cdot \text{s}^{-1}$
$C_s$	Reactant concentration	$\text{mol} \cdot \text{cm}^{-3}$
$X$	Associating coefficient of the solvent	1
$\mu$	Viscosity of the solvent	P
$M$	Relative molecular weight of the solute	$\text{g} \cdot \text{mol}^{-1}$
$V_b$	Molar volume of the solute	$\text{cm}^{-3} \cdot \text{mol}^{-1}$

## 2.3 Evaluation of the proximity channeling effect

The proximity channeling effect has been considered as a reason for the increased throughput in cascade reactions. It could facilitate the channeling of intermediates between the active sites rather than diffusing into the bulk solution. Although the exact mechanism of this channeling remains unclear, several mathematical methods have been successfully applied to explain this phenomenon [27,31].

Thus, a kinetic model describing the DKR reaction (as shown in Fig. 2) catalyzed by Pd/CALB-P is developed to evaluate the proximity channeling effect in EMHCs.

In a typical DKR process of  $(\pm)$ -1-PEA (Fig. 2(a)), CALB binds with  $(R)$ -1-PEA and transfers the acyl group from the acyl donor to  $(R)$ -1-PEA. The racemization reaction catalyzed by Pd clusters can achieve the interconversion of  $(R)$  and  $(S)$ -1-PEA. Owing to the continuous consumption of  $(R)$ -1-PEA by CALB,  $(R)$ -product tends to accumulate in the system. According to this principle, a kinetic model can be described as shown in Fig. 2(b), with additional assumptions made as: 1) the rate constants of the reversible racemization reactions are the same and 2)  $(S)$ -1-PEA will not be catalyzed by CALB. Therefore, the kinetic model can be developed as follows:

$$\frac{d[P]}{dt} = k_2[R]^2 + f_c k_1([S] - [R]), \quad (8)$$

$$\frac{d[R]}{dt} = k_1([S] - [R]) - f_c k_1([S] - [R]) - k_2[R]^2, \quad (9)$$

$$\frac{d[S]}{dt} = -k_1([S] - [R]), \quad (10)$$

where  $k_1$  and  $k_2$  refer to the rate constants of the racemization reaction catalyzed by Pd clusters and the resolution reaction catalyzed by CALB, respectively. An additional term  $f_c$  is introduced to indicate the contribution of proximity channeling.  $[R]$ ,  $[S]$  and  $[P]$  refer to the concentrations of  $(R)$ -substrate,  $(S)$ -substrate and  $(R)$ -product, respectively.

### 3 Results and discussion

#### 3.1 Calculation of $C_{WP}$ and $\eta$

Here, the internal diffusion of reactants within the catalyst carriers is first evaluated, where catalysts should be

treated as spherical particles to study this diffusion process (see section 2.1). Therefore, the  $C_{WP}$  and  $\eta$  of Pd/C and Novozyme 435 were calculated to investigate the internal diffusion limitations. According to Eqs. (1–7), the parameters to calculate  $C_{WP}$  and  $\eta$  can be classified into 3 categories: 1) parameters related to catalysts ( $\rho_c$ ,  $R$ ,  $\theta$ ,  $\tau$ ,  $r_e$ ); 2) parameters related to reaction ( $r'$  (obs),  $C_s$ ); 3) parameters related to diffusion ( $X$ ,  $\mu$ ,  $M$ ,  $V_b$ ). Here,  $R$  refers to the size of the catalyst particles, rather than that of micro or nano Pd contained in catalysts which will be discussed below. Furthermore, several characterizations were conducted to confirm the structure of the materials in this study (see electronic supplementary material (ESM) and Figs. S1–S3 (cf. ESM)).

Specifically, for Pd/C, where Pd NPs are loaded onto active carbon, the available data in previous studies can be referred to obtain these parameters. For example, Li et al. [19] used Pd/C to catalyze the racemization of  $(S)$ -1-PEA in toluene and the Sonogashira reaction in water, where parameters related to the reaction ( $r'$  (obs),  $C_s$ ) can be obtained from the experimental data of conversion or production rates. Parameters related to diffusion (such as  $X$ ,  $\mu$ ,  $M$ ,  $V_b$ ) can be obtained by detailed conditions in specific reaction systems. Besides, parameters related to catalysts ( $\rho_c$ ,  $R$ ,  $\theta$ ,  $\tau$ ,  $r_e$ ) can be obtained in several reported studies on Pd/C [32–34]. Therefore,  $C_{WP}$  and  $\eta$  could be calculated based on these available data and the results are listed in Table 2. All the values of parameters used to calculate  $C_{WP}$  and  $\eta$  are listed in Tables S1 and S2 (cf. ESM).

Actually, very few available data can be available to calculate parameters related to Novozyme 435 (such as  $\rho_c$ ,  $\theta$  and  $r_e$ ) because of the lack of structural characterizations of the immobilized enzyme catalysts, indicating that the  $C_{WP}$  of Novozyme 435 cannot be directly calculated. However, the  $\eta$  of Novozyme 435 can be obtained from the ratio of the apparent activity to the activity of free CALB in aqueous solution. This is because  $\eta$  is defined as the ratio of the observed activity to the intrinsic activity of catalysts, with an additional

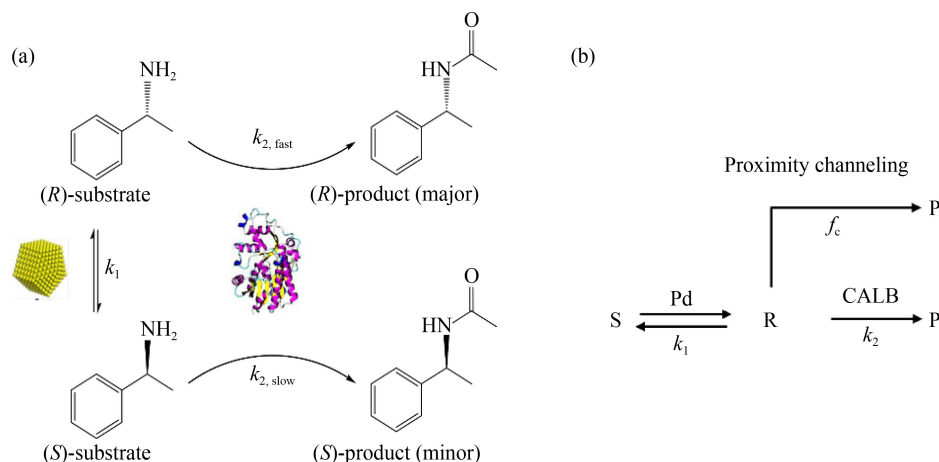


**Fig. 2** Schematics showing (a) the principles and (b) kinetic models of the DKR reaction catalyzed by CALB and Pd clusters.

**Table 2** Weisz–Prater parameters ( $C_{WP}$ ) and effectiveness factors ( $\eta$ ) of different catalysts

Catalyst	$C_{WP}$	$\eta$
Pd/C (in toluene)	0.0098	0.9993
Pd/C (in water)	0.0168	0.9988
Novozyme 435	20.8400	0.3300

assumption that the encapsulation in polymer will not affect the enzymatic activity. This assumption is rational according to Li's experiments [19,35] where the residual activity of CALB-P is nearly 90%. Therefore,  $C_{WP}$  can also be calculated according to Eqs. (2) and (3).

Furthermore, to demonstrate the difference of internal diffusion limitations in Pd/C and Novozyme 435, radar maps were drawn (Fig. 3). As shown in Fig. 3(a), the red arrow represents an increase in the internal diffusion effect with a decreased  $\eta$ . The  $\eta$  of Pd/C (in toluene and water) is nearly equal to 1, indicating that the internal diffusion of reactants in Pd/C is not dominant and can be ignored. However, the  $\eta$  of Novozyme 435 (close to the center of the radar map in Fig. 3(a)) is 0.33, indicating an obvious internal diffusion limitation existed in catalytic process. Figure 3(b) shows the radar map of  $C_{WP}$  where the red triangle indicates that  $C_{WP}$  is equal to 1 as a criterion of the internal diffusion limitation. The  $C_{WP}$  of Novozyme 435 is 20.84 (outside the triangle), while the  $C_{WP}$  of Pd/C is inside the triangle ( $<<1$ ), which is consistent with Fig. 3(a).

Besides, the particle size of Pd/C is valued as  $110\text{ }\mu\text{m}$  when calculating  $C_{WP}$ , while the size of Pd/CALB-P is at nanoscale. According to Eq. (1), the internal diffusion effect is significantly determined by  $R$ , the size of catalyst. Therefore, it can be inferred that the internal diffusion effect can be disregarded in Pd/CALB-P. Besides, in previous experiments, supported noble metal catalysts were generally observed to exhibit the size effect [36,37]. When the size of metal catalysts reduces from nanoscale to sub nanoscale, the activity of metal NPs may be significantly increased at relatively low temperatures, which was caused by the morphological change in metal NPs and the interactions between the metal NPs and matrix (such as the electron transfer and coordination

conditions). This phenomenon was also observed in Pd/CALB-P hybrid catalysts. For example, Li et al. [19] reported that the size of Pd NPs could be easily tuned from 0.8 to 2.5 nm by changing the concentration of precursors (see ESM) while the 0.8 nm Pd NPs was found to possess the highest activity in racemization of (S)-1-PEA. In addition, the average size of Pd in Pd/C was characterized to be 4.2 nm by transmission electron microscopy. Therefore, based on these results, it can be inferred that, for Pd NPs, the increased activity of Pd/CALB-P in the DKR process could be attributed to the size effect, rather than the internal diffusion limitation in Pd/C. In other words, the process catalyzed by Pd NPs tends to be reaction-limited while that catalyzed by Novozyme 435 tends to be diffusion-limited. From this perspective, the increased activity of Pd/CALB-P during the DKR process might be attributed to the size effect of Pd NPs and the decreased internal diffusion limitation compared with Novozyme 435.

### 3.2 Estimation of rate constants

According to Eqs. (8–10), the rate constants ( $k_1$ ,  $k_2$ ) and proximity effect factor ( $f_c$ ) are two necessary variables to evaluate the proximity channeling effect in Pd/CALB-P by kinetic modelling. Hence, based on available experimental data, the apparent rate constants are estimated to evaluate the contribution of  $f_c$  to the kinetics of the DKR.

Based on the fourth global assumption in section 2.1, racemization reactions catalyzed by Pd NPs are assumed to be first-order to substrates. Therefore, the evolution of the concentrations of  $[R]$  and  $[S]$  species in solution can be described by the following rate equations:

$$\frac{d[S]}{dt} = -k_1([S] - [R]), \quad (11)$$

$$\frac{d[R]}{dt} = k_1([S] - [R]), \quad (12)$$

where  $[S]$  and  $[R]$  are the concentrations of (S)- and (R)-1-PEA, respectively and  $k_1$  is the rate constant of the racemization reactions catalyzed by Pd NPs. By summing and subtracting Eqs. (11) and (12), the following

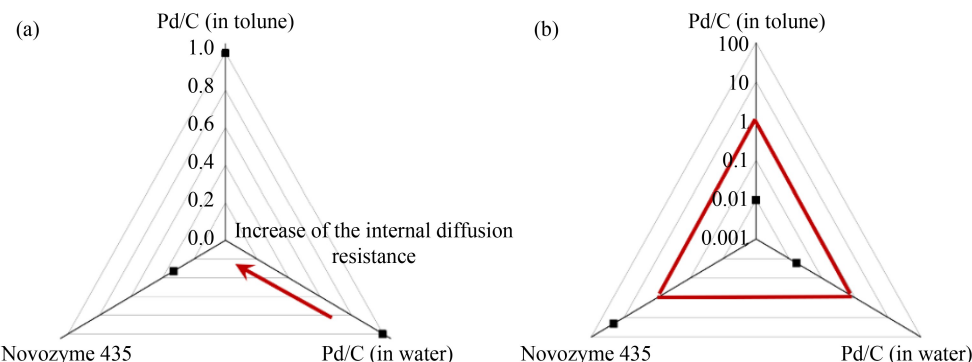


**Fig. 3** Radar maps illustrated the (a) effectiveness factor of internal diffusion  $\eta$  and (b) Weisz–Prater parameter  $C_{WP}$  of Pd/C and Novozyme 435.

equations can be obtained:

$$[S] + [R] = \text{const.} \quad (13)$$

$$E = \frac{[S] - [R]}{[S] + [R]}, \quad (14)$$

$$\frac{dE}{dt} = -2k_1 E, \quad (15)$$

where  $E$  refers to the value of the enantiomeric excess. The integral form of Eq. (15) can be written as follows:

$$\ln E_t = -2k_1 t + \ln E_0. \quad (16)$$

Using Eq. (16), the rate constant  $k_1$  can be estimated by the evolution of  $E$  over time during experiments.

To determine the reaction order of CALB to substrates, if it was a first-order reaction,  $\ln[1/(1-X)]$  would be linearly dependent on time, while if it was second-order reaction,  $X/(1-X)$  would be linearly dependent on time (see Eqs. (S1–S7), cf. ESM), where  $X$  is the conversion rate. Here, this assumption concerning the reaction order was proposed based on the simplification of the Michaelis–Menten equation when the concentration of substrates was relatively low. Following Li's experiments in kinetic resolution of  $(\pm)$ -1-PEA by CALB (Novozyme 435 and Pd/CALB-P) [19,35], the relationship between  $X$  and  $t$  was obtained, as shown in Fig. 4. The linearity obtained in Figs. 4(b) and 4(d) are higher than that in Figs. 4(a) and 4(c), for both of Pd/CALB-P and Novozyme 435,

indicating that the assumption of second-order is reasonable. Apart from the assumptions made in this study, it is notable that the relatively poor linearity in Figs. 4(c) and 4(d) may also be resulted from the data errors in previous experimental study. Thus, rate constant  $k_2$  can be estimated using the slope of  $X/(1-X)$  over  $t$ . The estimation values of  $k_1$  and  $k_2$  are listed in Table S3 (cf. ESM).

With the estimated apparent rate constants, the contribution of the proximity effect factor,  $f_c$ , to the kinetics of the DKR can be determined by the numerical solution of Eqs. (8–10), as illustrated in Fig. 5. When there is no proximity effect (the dashed and green line in Fig. 5) in Pd/C + Novozyme 435 (as is supposed to) and Pd/CALB-P, the throughput of Pd/CALB-P is relatively higher, indicating that the proximity effect is not the only reason for the enhanced throughput and this increase may originate from the size effect of Pd NPs or the decreased internal diffusion limitation compared with Novozyme 435. However, when  $f_c$  changes from 0 to 1 in Pd/CALB-P, an increase in  $[P]$  is observed, confirming that the contribution of the proximity effect in this model can accelerate the apparent kinetics and improve the throughput of cascade reactions.

### 3.3 Fitting of the kinetic model

The proximity effect factor,  $f_c$ , indicates the contribution

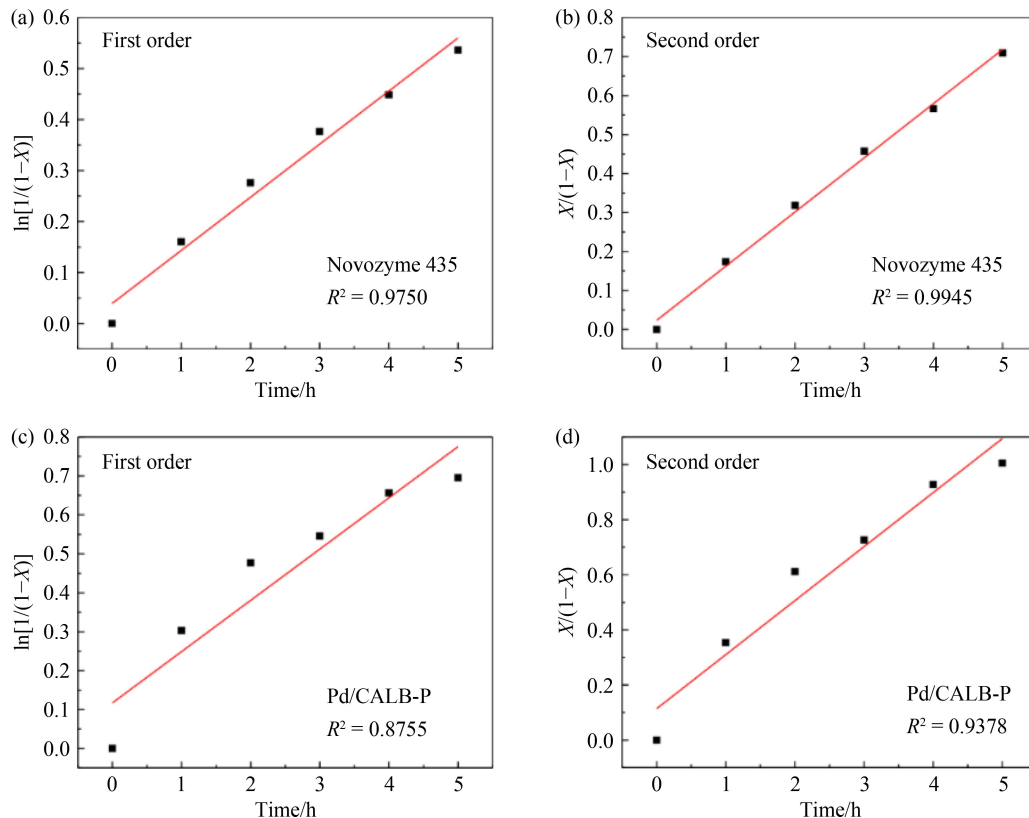


**Fig. 4** Verification of the reaction order of (a, b) Novozyme 435 and (c, d) Pd/CALB-P to the R-substrate when assuming (a, c) first order and (b, d) second order, respectively.

of the proximity channeling to the overall kinetics of cascade reactions, which is similar to the efficiency factor of internal diffusion  $\eta$ . To ensure the integrity and generality of this kinetic model, it is necessary to fit parameters to experimental data. Hence, the parameters ( $k_1$ ,  $k_2$  and  $f_c$ ) in this kinetic model (Eqs. (8) to (10)) are fitted to the experimental DKR data [19] catalyzed by Pd/CALB-P and Pd/C + Novozyme 435 using the least square method.

Fitting values of the kinetic parameters and fitting curves of the DKR reaction are illustrated in Table 3 and Fig. 6, respectively. According to Table 3, there exists a significant difference in the proximity effect factor  $f_c$  between Pd/CALB-P and Pd/C + Novozyme 435, where the fitting results are evaluated at the upper and lower boundaries, respectively. The result indicates that the contribution of the proximity channeling effect to the DKR kinetics is prominent in Pd/CALB-P. However, it is

practically futile in the combination of Pd/C and Novozyme 435.

As listed in Table 3, the  $k_2$  of Pd/CALB-P (valued as 13.6) is approximately 23 times than that of Novozyme 435 (valued as 0.6), while there is no obvious difference in  $k_1$  between Pd/CALB-P (valued as 0.37) and Pd/C (valued as 0.13). This result may again indicate that the catalytic process of Novozyme 435 is internal diffusion-limited and it is a reaction-controlled process for Pd/C and Pd/CALB-P, which correlates with the calculated results in section 3.1.

## 4 Conclusions

The diffusion process in EMHCs is investigated using synthesized Pd/CALB-Pluronic conjugates and the combination of commercial catalysts (Pd/C and Novozyme 435) as models. The effect of internal diffusion and proximity channeling in these catalysts are evaluated to reflect the diffusion of reactants from the bulk solution to active sites and the diffusion of intermediates between active sites, respectively. By calculating the Weisz–Prater parameter and the efficiency factor of internal diffusion, it was found that there existed an obvious internal diffusion limitation in Novozyme 435 while this effect could be ignored in Pd/CALB-P and Pd/C. By developing a kinetic model to describe the DKR reaction and fitting it to the experimental data, it was proved that the proximity effect existing in Pd/CALB-P would contribute to an increased throughput in apparent kinetics. Therefore, based on these calculation results, the enhanced catalytic efficiency of Pd/CALB-P can be attributed to the following reasons: 1) the decreased internal diffusion limitation in Pd/CALB-P, compared with Novozyme 435; 2) the size effect of metal NPs, compared with Pd/C; 3) the proximity effect of active sites in a confined environment.

**Acknowledgements** This work was supported by the Beijing Natural Science Foundation (No. JQ18006), and the National Natural Science Foundation of China (Grant Nos. 21878174, 2191101041).

**Electronic Supplementary Material** Supplementary material is available in the online version of this article at <https://dx.doi.org/10.1007/s11705-022-2144-4> and is accessible for authorized users.

## References

- Choi J M, Han S S, Kim H S. Industrial applications of enzyme biocatalysis: current status and future aspects. *Biotechnology Advances*, 2015, 33(7): 1443–1454
- Sandoval B A, Hyster T K. Emerging strategies for expanding the toolbox of enzymes in biocatalysis. *Current Opinion in Chemical Biology*, 2020, 55(1): 45–51
- Taguchi S. Designer enzyme for green materials innovation:

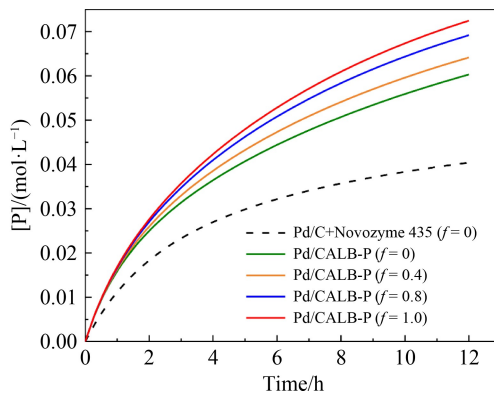


**Fig. 5** Numerical solutions of the DKR reaction model for Pd/C + Novozyme 435 (dashed line) and Pd/CALB-P (solid line) with different fractions of the proximity channeling effect.

**Table 3** Fitting values of kinetic parameters in the DKR reaction model

Catalyst	$k_1$	$k_2$	$f_c$
Pd/C + Novozyme 435	0.13	0.60	0
Pd/CALB-P	0.37	13.60	1

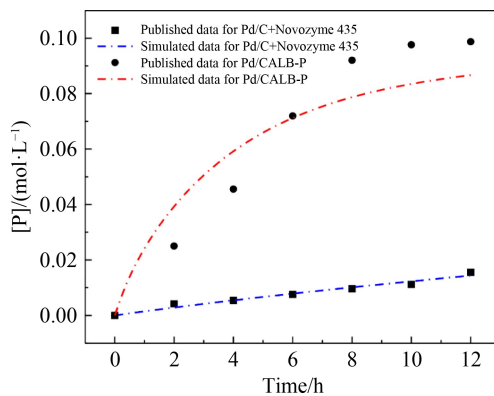


**Fig. 6** Fitting of the DKR reaction model to the experimental data reported for the Pd/C + Novozyme 435 and Pd/CALB-P.

- lactate-polymerizing enzyme as a key catalyst. *Frontiers of Chemical Science and Engineering*, 2017, 11(1): 139–142
- 4. Gao C, Lyu F, Yin Y. Encapsulated metal nanoparticles for catalysis. *Chemical Reviews*, 2021, 121(2): 834–881
  - 5. Jiao L, Yan H, Wu Y, Gu W, Zhu C, Du D, Lin Y. When nanozymes meet single-atom catalysis. *Angewandte Chemie International Edition*, 2020, 59(7): 2565–2576
  - 6. Debecker D P, Smeets V, Van der Verren M, Arango H M, Kinnaer M, Devred F. Hybrid chemoenzymatic heterogeneous catalysts. *Current Opinion in Green and Sustainable Chemistry*, 2021, 28(1): 100437
  - 7. Denard C A, Hartwig J F, Zhao H. Multistep one-pot reactions combining biocatalysts and chemical catalysts for asymmetric synthesis. *ACS Catalysis*, 2013, 3(12): 2856–2864
  - 8. Huang X, Cao M, Zhao H. Integrating biocatalysis with chemocatalysis for selective transformations. *Current Opinion in Chemical Biology*, 2020, 55: 161–170
  - 9. Cao Y, Ge J. Hybrid enzyme catalysts synthesized by a de novo approach for expanding biocatalysis. *Chinese Journal of Catalysis*, 2021, 42(10): 1625–1633
  - 10. Cortes-Clerget M, Akporji N, Zhou J, Gao F, Guo P, Parmentier M, Gallou F, Berthon J Y, Lipshutz B H. Bridging the gap between transition metal- and bio-catalysis via aqueous micellar catalysis. *Nature Communications*, 2019, 10(1): 2169
  - 11. Li X, Cao X, Xiong J, Ge J. Enzyme–metal hybrid catalysts for chemoenzymatic reactions. *Small*, 2020, 16(15): 1902751
  - 12. Ye R, Zhao J, Wickemeyer B B, Toste F D, Somorjai G A. Foundations and strategies of the construction of hybrid catalysts for optimized performances. *Nature Catalysis*, 2018, 1(5): 318–325
  - 13. Thalen L K, Zhao D, Sortais J B, Paetzold J, Hoben C, Backvall J E. A chemoenzymatic approach to enantiomerically pure amines using dynamic kinetic resolution: application to the synthesis of norsertraline. *Chemistry (Weinheim an der Bergstrasse, Germany)*, 2009, 15(14): 3403–3410
  - 14. Filice M, Marciello M, del Puerto Morales M, Palomo J M. Synthesis of heterogeneous enzyme–metal nanoparticle biohybrids in aqueous media and their applications in C–C bond formation and tandem catalysis. *Chemical Communications*, 2013, 49(61): 6876–6878
  - 15. Gustafson K P J, Gorbe T, de Gonzalo G, Yuan N, Schreiber C L, Shchukarev A, Tai C, Persson I, Zou X, Backvall J E. Chemoenzymatic dynamic kinetic resolution of primary benzylic amines using Pd-0-CALB CLEA as a biohybrid catalyst. *Chemistry (Weinheim an der Bergstrasse, Germany)*, 2019, 25(39): 9174–9179
  - 16. Zhang N, Hubner R, Wang Y, Zhang E, Zhou Y, Dong S, Wu C. Surface-functionalized mesoporous nanoparticles as heterogeneous supports to transfer bifunctional catalysts into organic solvents for tandem catalysis. *ACS Applied Nano Materials*, 2018, 1(11): 6378–6386
  - 17. Wang Y, Zhang N, Zhang E, Han Y, Qi Z, Ansorge-Schumacher M B, Ge Y, Wu C. Heterogeneous metal-organic-framework-based biohybrid catalysts for cascade reactions in organic solvent. *Chemistry (Weinheim an der Bergstrasse, Germany)*, 2019, 25(7): 1716–1721
  - 18. Verho O, Backvall J E. Chemoenzymatic dynamic kinetic resolution: a powerful tool for the preparation of enantiomerically pure alcohols and amines. *Journal of the American Chemical Society*, 2015, 137(12): 3996–4009
  - 19. Li X, Cao Y, Luo K, Sun Y, Xiong J, Wang L, Liu Z, Li J, Ma J, Ge J, Xiao H, Zare R N. Highly active enzyme–metal nano-hybrids synthesized in protein–polymer conjugates. *Nature Catalysis*, 2019, 2(8): 718–725
  - 20. Engstrom K, Johnston E V, Verho O, Gustafson K P J, Shakeri M, Tai C W, Bäckvall J E. Co-immobilization of an enzyme and a metal into the compartments of mesoporous silica for cooperative tandem catalysis: an artificial metalloenzyme. *Angewandte Chemie International Edition*, 2013, 52(52): 14006–14010
  - 21. Gustafson K P J, Lihammar R, Verho O, Engstrom K, Backvall J E. Chemoenzymatic dynamic kinetic resolution of primary amines using a recyclable palladium nanoparticle catalyst together with lipases. *Journal of Organic Chemistry*, 2014, 79(9): 3747–3751
  - 22. Zhang X, Jing L, Chang F, Chen S, Yang H, Yang Q. Positional immobilization of Pd nanoparticles and enzymes in hierarchical yolk-shell@shell nanoreactors for tandem catalysis. *Chemical Communications*, 2017, 53(55): 7780–7783
  - 23. Idan O, Hess H. Diffusive transport phenomena in artificial enzyme cascades on scaffolds. *Nature Nanotechnology*, 2012, 7(12): 769–770
  - 24. Idan O, Hess H. Origins of activity enhancement in enzyme cascades on scaffolds. *ACS Nano*, 2013, 7(10): 8658–8665
  - 25. Tsitkov S, Pesenti T, Palacci H, Blanchet J, Hess H. Queueing theory-based perspective of the kinetics of “channeled” enzyme cascade reactions. *ACS Catalysis*, 2018, 8(11): 10721–10731
  - 26. Zhang Y, Hess H. Toward rational design of high-efficiency enzyme cascades. *ACS Catalysis*, 2017, 7(9): 6018–6027
  - 27. Zhang Y, Tsitkov S, Hess H. Proximity does not contribute to activity enhancement in the glucose oxidase-horseradish peroxidase cascade. *Nature Communications*, 2016, 7(1): 13982
  - 28. Breveglieri F, Mazzotti M. Role of racemization kinetics in the deracemization process via temperature cycles. *Crystal Growth & Design*, 2019, 19(6): 3551–3558
  - 29. Rahmani E, Rahmani M. Catalytic process modeling and sensitivity analysis of alkylation of benzene with ethanol over MIL-101(Fe) and MIL-88(Fe). *Frontiers of Chemical Science and Engineering*, 2020, 14(6): 1100–1111
  - 30. Liu Y, Qu J, Wu X, Zhang K, Zhang Y. Reaction kinetics and internal diffusion of Zhundong char gasification with CO<sub>2</sub>. *Frontiers of Chemical Science and Engineering*, 2021, 15(2): 373–383
  - 31. Li G, Zhang C, Xing X. A kinetic model for analysis of physical tunnels in sequentially acting enzymes with direct proximity channeling. *Biochemical Engineering Journal*, 2016, 105(1): 242–248
  - 32. Liang K. Industrialized study of Pd/C catalyst and its applying in catalytic transfer hydrogenation. Dissertation for the Doctoral Degree. Lanzhou: Lanzhou University, 2008
  - 33. Zhu L. Study on deactivation and regeneration of Pd/C catalysts for PTA hydrofining. Dissertation for the Master Degree. Shanghai: East China University of Science and Technology,

- 2015: 20–21
- 34. Yang Y. Preparation and characterization of Pd/C catalysts and their application in hydrogenation of dehydrodibenzylbiotin-methyl ester. Dissertation for the Master Degree. Hangzhou: Zhejiang University of Technology, 2013
  - 35. Li X. Construction and application of enzyme–metal hybrid catalysts with controllable metal nanoparticle size. Dissertation for the Doctoral Degree. Beijing: Tsinghua University, 2020
  - 36. Bai L, Wang X, Chen Q, Ye Y, Zheng H, Guo J, Yin Y, Gao C. Explaining the size dependence in platinum-nanoparticle-catalyzed hydrogenation reactions. *Angewandte Chemie International Edition*, 2016, 55(50): 15656–15661
  - 37. Dong C, Lian C, Hu S, Deng Z, Gong J, Li M, Liu H, Xing M, Zhang J. Size-dependent activity and selectivity of carbon dioxide photocatalytic reduction over platinum nanoparticles. *Nature Communications*, 2018, 9(1): 1252